16th World Conference on Earthquake, 16WCEE 2017
Santiago Chile, January 9th to 13th 2017
Paper N° 2466 (Abstract ID)
Registration Code: S-K1464748820

Assessment of Seismic Vulnerability of Historic Buildings Based on their Current Condition Captured by Laser Scans and Retrofit Strategies

Shakhzod Takhirov[(1)], Amir Gilani[(2)], Brian Quigley[(3)], Liliya Myagkova[(4)]

[(1)] *Structures Laboratory – Eng. Manager, University of California at Berkeley, Berkeley, USA, takhirov@berkeley.edu*
[(2)] *Senior Associate, Miyamoto International, Inc., Sacramento, USA, agilani@miyamotointernational.com*
[(3)] *BNZ, Tashkent, Uzbekistan, hitg.eurasia@gmail.com*
[(4)] *Smart Scanning Solutions, LLC, Tashkent, Uzbekistan, myagkova_liliya@mail.ru*

Abstract

The technology of high-definition laser scanning is an essential tool for accurate non-destructive three-dimensional measurements of structures. The object's geometry is captured as a collection of points which is called a "point cloud". The research team used this technology and conducted an extensive laser scanning of three major historic monuments in Shakhrisabz, Uzbekistan. The city is located in southern Uzbekistan approximately 80 km south of Samarkand, Uzbekistan. Once a major city of Central Asia, it is primarily known today as the birthplace of 14th century Turco-Mongol conqueror Timur. The scanned monuments are from the Timurid Dynasty era and they are on the UNESCO World Heritage List. The Timur's Summer Palace, the Ak-Saray Palace (White Palace) was planned as the most grand of all Timur's constructions and it was started in 1380. Unfortunately, only traces of its gigantic 65 m gate-towers survived. The Kok Gumbaz (Blue Dome) Mosque was built in 1437 and underwent several restorations and reinforcement efforts. East of the Kok Gumbaz, there is another mausoleum complex called Dorus-Saodat (Seat of Power and Might), which contains the Tomb of Jehangir, Timur's eldest and favorite son. A detailed finite element model of each monument was generated from the as-found geometry captured by laser scans. To monitor the buildings' possible settlement due to poor soil conditions, special high-resolution laser targets were permanently installed. The physical properties of the monuments were investigated by material tests of the major components recovered from the historic sites. The calibrated models were used for comprehensive seismic analysis of the monuments and its components. All current reinforcement details were accounted for in the numerical models. Based on the results of numerical simulations, recommendations on further reinforcement of the historic monuments were developed.

Keywords: seismic performance; numerical modeling and time history analysis; time history analysis; laser scanning; seismic retrofit of historic buildings

1. Introduction

The technology of high-definition laser scanning is an essential tool for accurate non-destructive three-dimensional measurements of structures. The object's geometry is captured as a collection of points, which is called a "point cloud". The research team used this technology and conducted an extensive laser scanning program of many historic monuments in Uzbekistan. The program started in 2013 from scanning the famous Registan ensemble in Samarkand [1]. Later in 2015, it was expanded to more cities and monuments and the laser scanning was conducted in Tashkent, Bukhara, Samarkand and Shakhrisyabz. Because of size limitations of this paper, mainly results of a major historic monument in Shakhrisyabz, Uzbekistan are discussed herein in details. Uzbekistan's location on Earth and the Shakhrisyabz's location on the country map are shown in Fig. 1. The city is located in southern Uzbekistan approximately 80 km south of Samarkand, Uzbekistan. Once a major city of Central Asia, it is primarily known today as the birthplace of 14th century Turco-Mongol conqueror Timur. The scanned monument, the Kuk Gumbaz (Blue Dome) Mosque, is from the Timurid Dynasty era and it is on the UNESCO World Heritage List. The monument was built in 1437 and over the years underwent several restorations and reinforcement efforts.

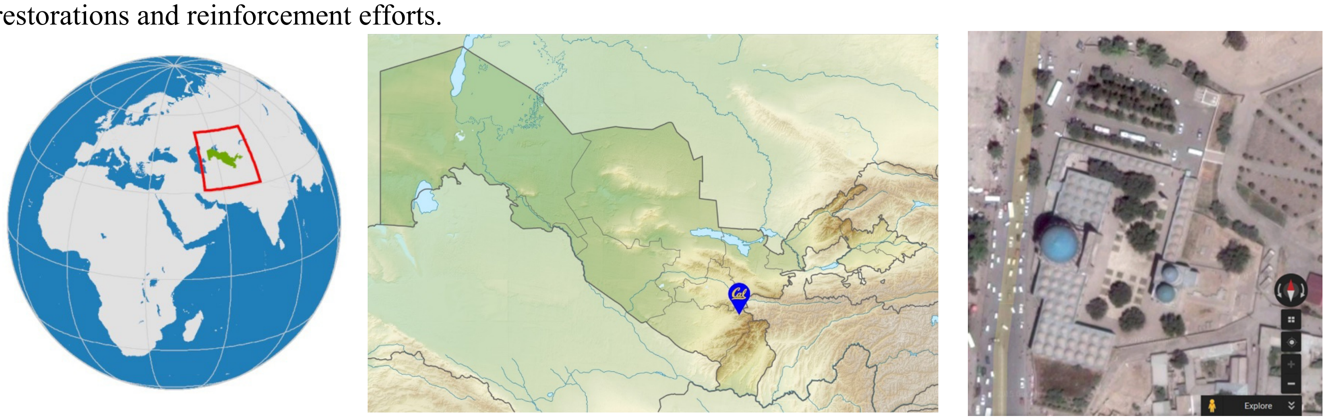

a) Uzbekistan's location   b) Location of Shakhrisyabz on Uzbekistan's map   c) Google satellite view of monument

Fig. 1 – Monument's geographic location

2. Laser scanning

The historic monument was scanned from 13 stations as presented in Fig. 2. The scans were conducted on August 13, 2015. The stitching was performed in Cyclone [1] and error did not exceed 3 mm for all scans used in the final registration.

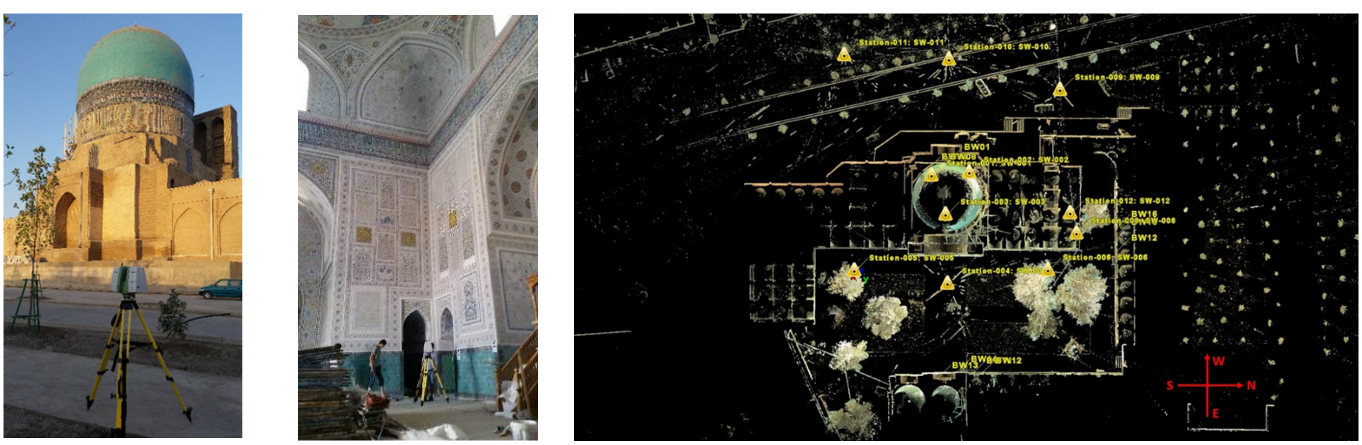

a) Exterior station   b) Interior station   c) Final registration of laser scans in TruSpace (coordinate system is presented in red)

Fig. 2 – Locations of scanning stations

The monument was scanned from outside, inside of the main hall, and inside of a stairway with a large crack between the portal and the main structure. Some of scan stations are shown in Fig. 2a and Fig. 2b. A resultant point cloud of the mosque stitched from the scans captured from the thirteen scanner locations is presented in Fig. 3.

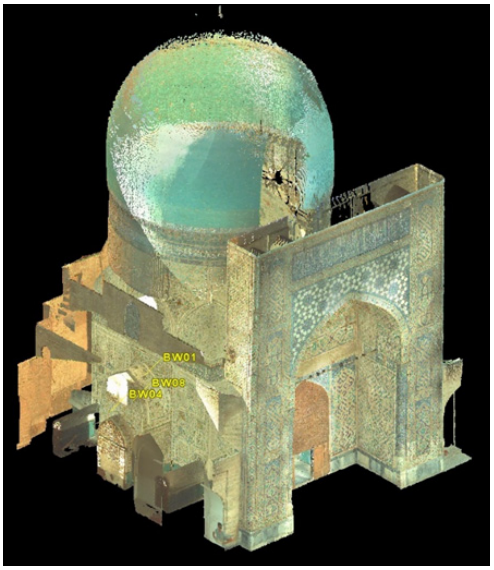

a) Stitched point cloud: isometric view

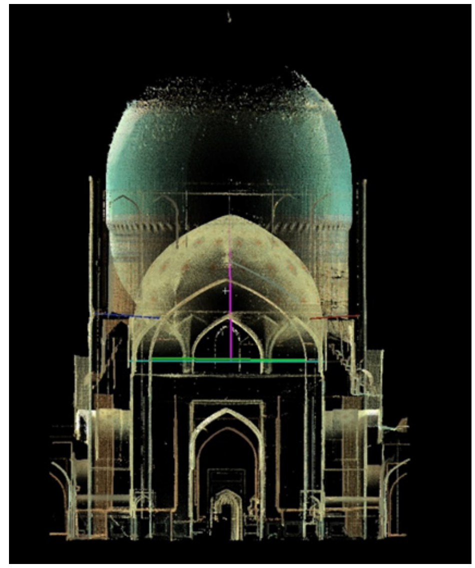

b) Stitched point cloud: front view

Fig. 3 – Resultant point cloud of mosque

3. Mosque's Existing Structural Reinforcement

The monument was under reconstruction and renovation at the time of the laser scanning of the site. The final painting was ongoing inside of the main hall of the mosque and the project associated with replacing of the old tiles on the main globe was in progress. The restoration activities did not include structural strengthening of any kind. The structural reinforcement of the monument was performed earlier with the major structural components presented in Fig. 4. As shown in Fig. 5a the inner globe was also reinforced by a steel rod installed parallel to the portal at the bottom of the globe. This rod was suspended from another steel rod hanging from the top. Since a large crack separating the portal from the main structure was developed earlier, the portal was pulled back to the main structure by means of steel angles which were pretensioned in place by turnbuckles, as shown in Fig. 5b. In addition, the left and right arcs of the portal were pretensioned to each other via a steel rod as presented in Fig. 5c. All exposed reinforcement was captured by a laser scanner which is summarized in Table 1. The cross sections of steel rods presented in this table were estimated from a point cloud.

From analysis of the point cloud it was concluded that reinforcement rods did not reveal any sagging. This serves as evidence that the tension force was still present in the rods. One of the pretension rods applied force in weak direction of the reinforcement member (web of a double channel) that resulted in plastic deformations of the double channel. The latter was installed at Elevation 3 as shown in Fig. 4b. It was most likely related to a mistake in the engineering detailing of the way the reinforcement needed to be installed in the monument. Because this reinforcement could not serve its purpose, it was not included in the model.

It worthy to note that the engineering detailing of the existing reinforcement was not done in a proper way. The current reinforcement attracts the forces and creates stress concentration points. Localized failures of masonry around the attachment points were observed at several locations throughout the monument. Therefore, these connection details need to be redesigned to distribute forces where the brace comes in contact with the masonry.

a) North side – upper angle (Elevation 1)

b) North side – double channels with prestress bars parrallel to portal's face (Elevation 3)

c) South side – upper angle (Elevation 1)

d) Double channels with prestress bars parrallel to portal's face (Elevation 3)

e) North side's I-beams orthogonal to portal's face (Elevation 2)

f) South side's angles orthogonal to portal's face (Elevation 2)

Fig. 4. Existing reinforments connecting portal to the main structure

Table 1 – Elevations where reinforcement was installed

Elevation No	**Z coordinate, m**	**Note**	**Description of structural member and size**
1	14.62	Portal to main structure at close to 45 degrees to E-W axis	Steel angle with a turnbuckle
2	12.36	Portal to main structure in E-W axis	Double I-beam
3	11.93	Portal to main structure in E-W axis and tensión rod through portal in S-N axis	Double channel
4	11.84	Tension bar between two arcs of main portal	26 mm steel bar
5	11.82	Tension bar at bottom of inner globe	29 mm steel bar

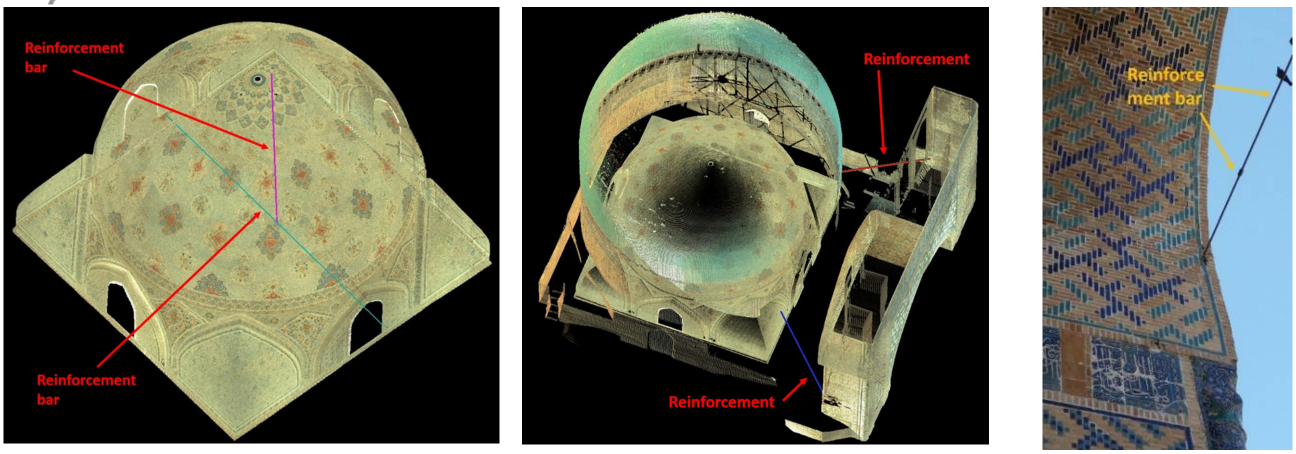

a) Reinforcement in inner globe b) Reinforcement between portal and main structure c) Rod between arcs of portal

Fig. 5 – Major pre-existing reinforcements of mosque

4. Mosque's Structural Anomalies

The monument's point cloud was investigated for anomalies. The main portal was investigated for its inclination from a vertical plane passing through the bottom of both piers. A color map of the inclinations is presented in Fig. 6a. The color map shows that the portal's inclination increases from south to north with the maximum differential displacement of 0.6m at the top north corner. To ensure that this degree of inclination of the portal is not progressing, a periodic monitoring by laser scanning was recommended. It was also advised to proceed with the installation of laser targets to increase accuracy of monitoring.

The same inclination for two vertical slices of the portal is presented in Fig. 6b. The cyan line (at Z = 14.62 m) corresponds to Elevation 1 where one type of reinforcement was installed. Since the slope of the slice (plots on the left side) does not change after this elevation, most likely the reinforcement is not effective and does not provide enough support to prevent continuous leaning of the portal. Another major conclusion was drawn from the Fig. 6b, that the residual drift of the structure remains the same from about 4 m to the top of the portal and this elevation coincides with the starting elevation of the crack that essentially separated the portal from the main structure.

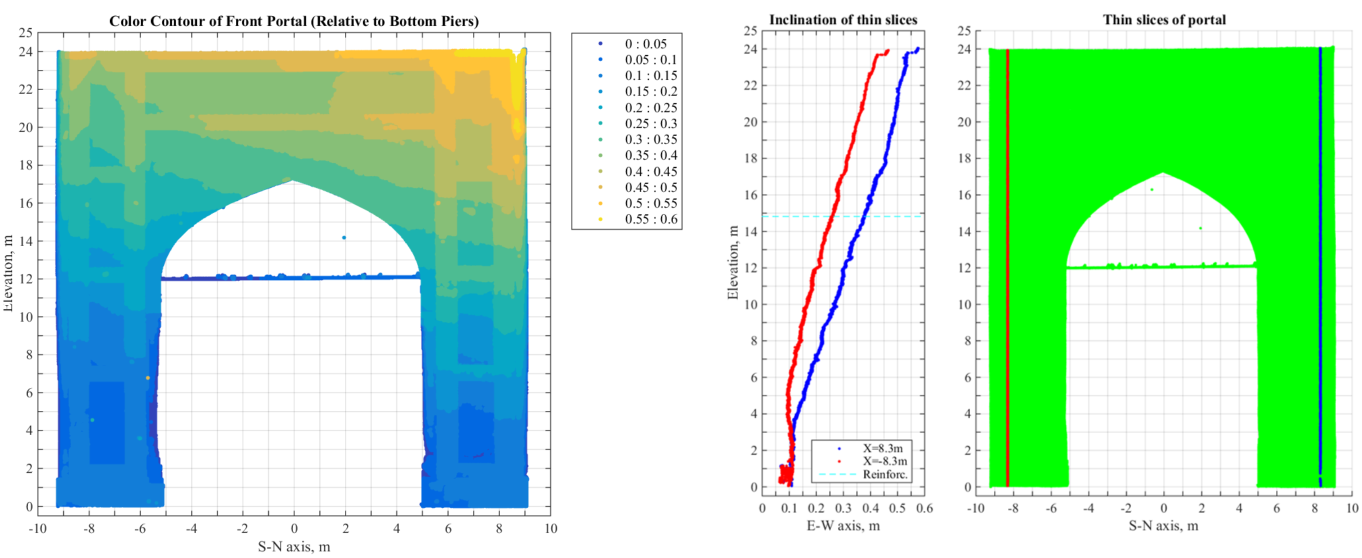

a) Color map of the portal's inclinations b) Two vertical slices showing portal's inclination at 8.3 m (blue) and -8.3 m (red) from its center

Fig. 6 – Major pre-existing reinforcements of mosque

Structural anomalies of the inner globe in the main structure shown in Fig. 7a were also studied. The color map of the inner globe's elevations is presented in Fig. 7b. The dashed lines show elevations with 1-meter increments and in many cases the color map for each elevation range have some deviations from the dashed lines. This shows imperfections of the globe. To ensure that the imperfections are not changing over time, a periodic monitoring by laser scanning was recommended. Two slices in S-N and E-W axes were cut from the inner globe as presented in Fig. 8a. These slices are plotted in Fig. 8b which shows that a slice at Y=0 m is lower on the left (south side) at elevation close to 14.8 m.

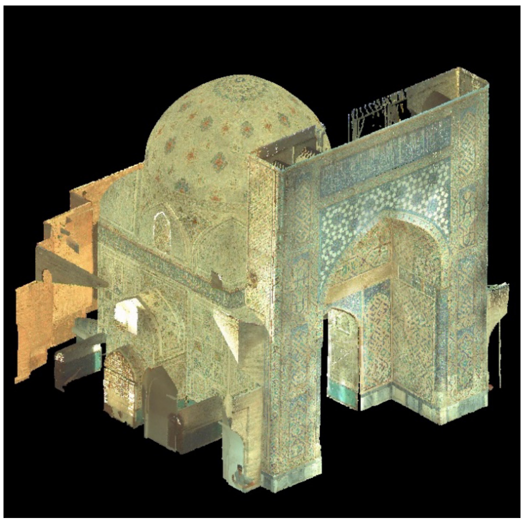

a) Inner globe of the main structure

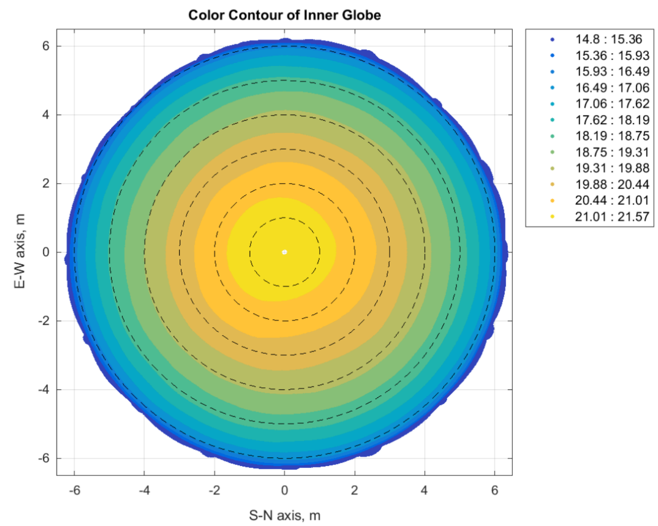

b) Color map of the inner globe's elevations

Fig. 7 – Current imperfections of inner globe

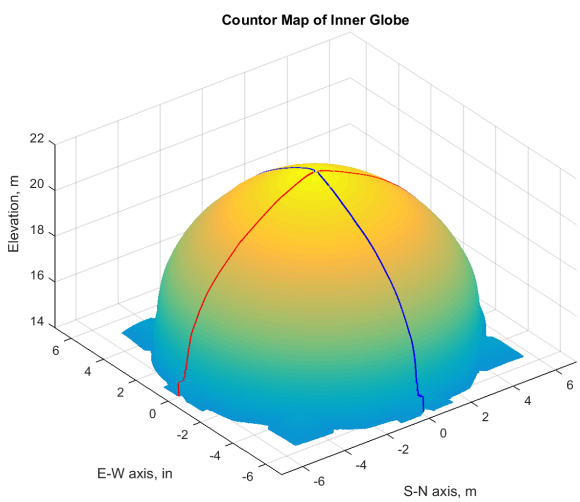

a) Two slices at 90 degrees to each other

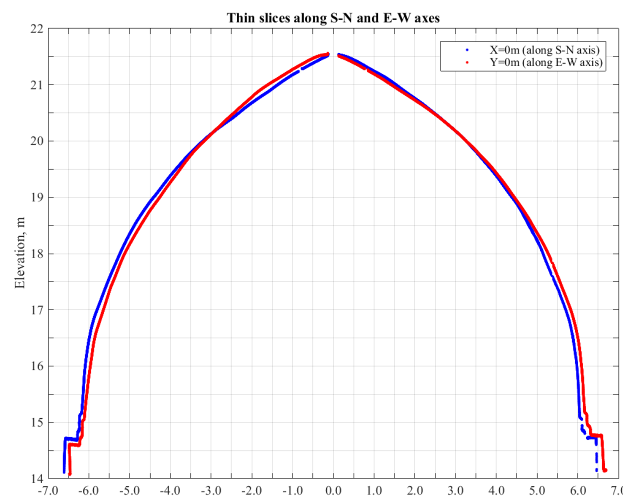

b) Sagging on east side of the inner globe (the red points are lower than the blue points at the plot's bottom – left side)

Fig. 8 – Sagging on east side of inner globe estimated from two vertical slices

The horizontal slices of the north pier and the stairway with a long crack between the portal and the main structures are shown in Fig. 9. The scanner was installed at several elevations of the stairway with one of them shown in Fig. 9a. These scans were also stitched with the main registration. The view of the stairway's point cloud is shown in Fig. 9b. The horizontal slices at several elevations of the stairway are presented in Fig. 9c. A similar, but smaller crack, was observed inside of the south pier of the portal.

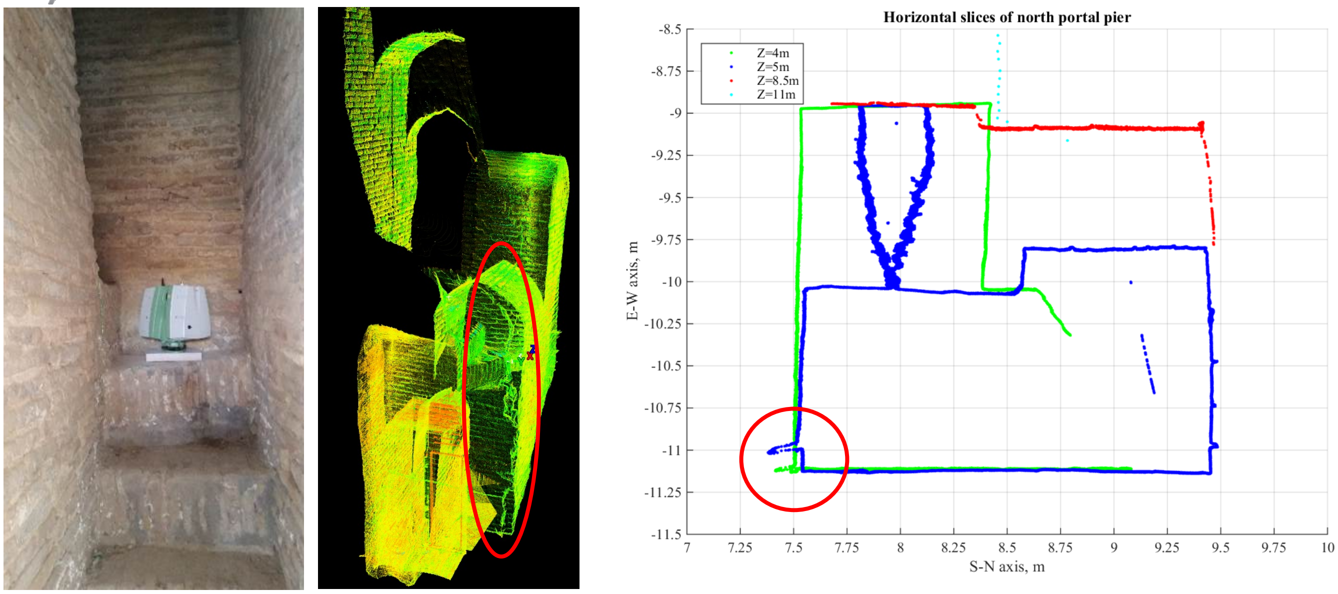

a) Scan station in stairway with a crack

b) Point cloud of the crack (inside of red oval)

c) Slices showing that the crack in the red circle propogates from elevation Z=4 m in a 2 m by 2 m stairway

Fig. 9 – Continuous crack in a narrow stairway (north pier of portal)

5. Geometry and Material Properties of Finite Element Model

The geometry of the finite element model was generated from the point cloud. All major imperfections and existing reinforcements were included into the geometry of the model. Numerical modelling and subsequent analysis was conducted in SAP2000 [3]. Since the crack in the north pier (shown in Fig. 9b and 9c) extends all the way to the top of the portal and a similar (but smaller) crack was observed inside of the pier on south side of the portal, a seismic performance of the portal was considered separately of that of the main structure. Since the main structure represents a boxed construction and as such, is much stiffer than the portal, it was assumed that the reinforcement between the portal and the main structure is attached to an absolutely rigid structure. The tension bar between the north and south arcs of the main portal was modelled in SAP2000 [3] as a steel frame (in SAP2000 terminology) with a round cross section. The reinforcement restraining the portal to the main structure was modelled as steel frame (SAP2000 terminology) with a shape of the structural angle. The geometry of the portal without reinforcements presented in Fig. 10 shows different portions of the portal in different colors.

The model was expanded to more complex model that included the main structure, the globes and the portal. Due to the limitations of this paper, only numerical results for the portal are presented here.

Since there is a very large variability in the material properties of masonry walls [1, 4-7], material tests were conducted on a brick recovered from the site. The material properties were homogenized in order to come up with the effective properties of a brick and mortar composite structure [8]. The numerical simulations of seismic impact were conducted by utilizing the Gazli 1976 earthquake from the PEER NGA Strong Motion Database [9]. This record is recommended for use by the structural code of Uzbekistan. The model was excited in all three principal directions. As a starting point, the simulations were limited to the elastic case.

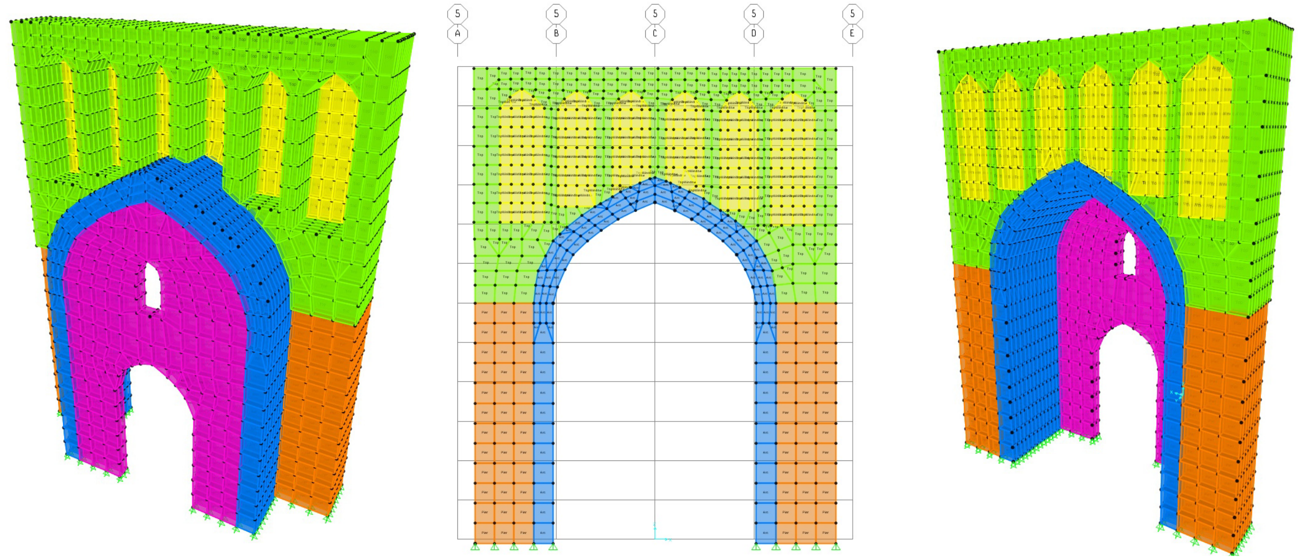

a) Rear view b) XZ view c) Front view

Fig. 10 – Different views of finite element model (reinforcement is not shown)

The material properties of the bricks from similar historic monuments were estimated earlier [1] by material tests. Test specimens were bored out from a brick as presented in Fig. 11a and tested in an Universal Test Machine under compression load (shown in Fig. 11b). The compression tests show that the stress versus strain curves for both longitudinal and transversal strains are quite linear all the way till failure of the test specimen as presented in Fig. 11c. In addition to the compression tests, a number of split tests were also conducted on the specimens extracted from the brick.

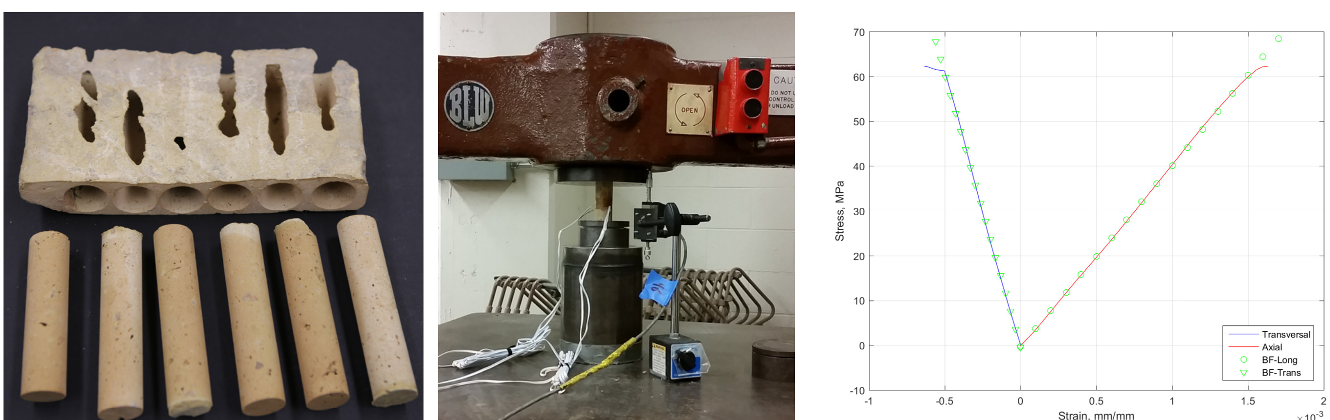

a) Test specimens b) Test in progress c) Test results: stress versus longitudinal and transversal strains

Fig. 11 – Bricks' material tests

6. Results of Numerical Analysis

The geometry of the finite element model was generated from the point cloud. All major imperfections and existing reinforcements were included into the model's geometry. Numerical modelling and subsequent analysis was conducted in SAP2000 [3]. Since the crack in the north pier (shown in Fig. 9) extends all the way to the top of the portal and a similar (but smaller) crack was observed in the pier on south side of the portal, it was assumed that the portal had separated from the main structure. As such, a very small interaction of the portal with the main structure is expected. Hence, a seismic performance of the portal itself was studied in details.

The seismic performance of the monument was evaluated by following requirements of the structural code of Uzbekistan [10]. Based on the code requirements, the strong motion recorded during the 1976 Gazli earthquake shall be utilized in the time history analysis. The Gazli strong motion needs to be scaled to account for expected seismic intensity of potential earthquakes in the region. The seismic excitations were imposed in all three directions. As the most critical directions, the spectral accelerations and the time histories for both horizontal components are presented in Fig. 13.

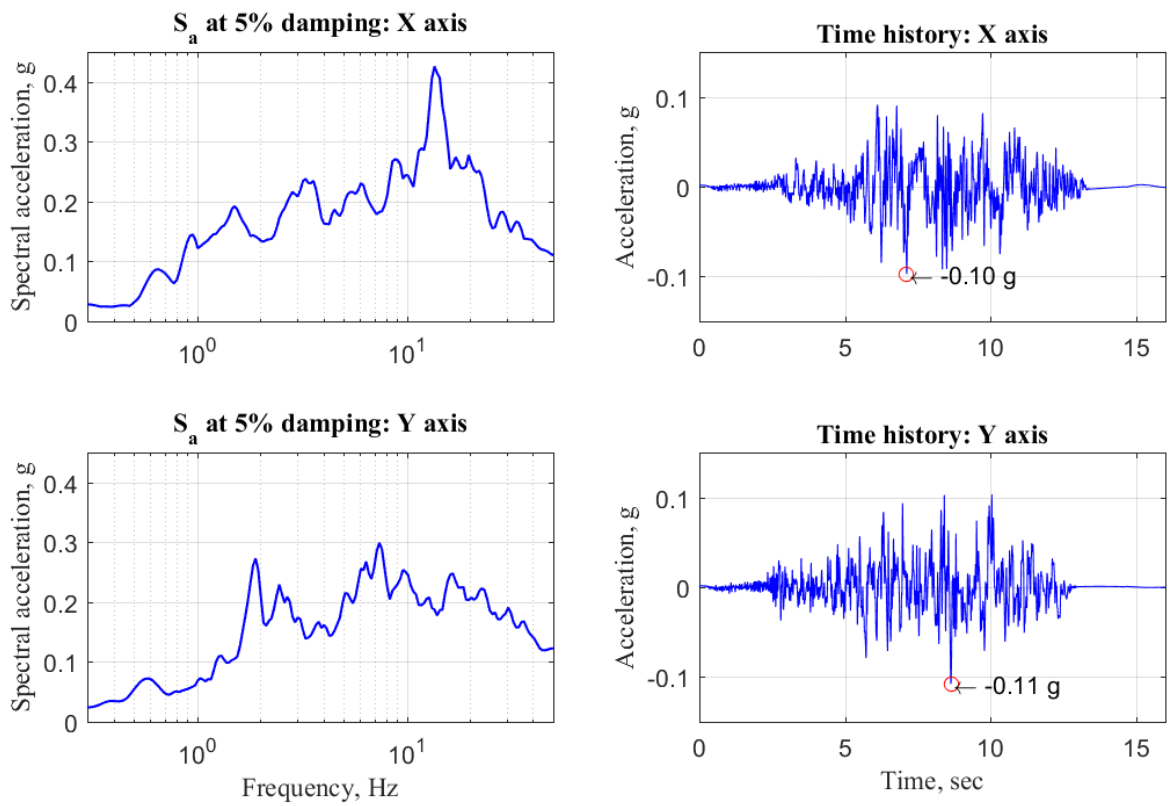

Fig. 13 – Two horizontal components of Gazli records scaled for Shakhrisyabz

To investigate the effectiveness of the current reinforcement and in order to study other options, four models with different reinforcement were considered as presented in Table 2. As it can be seen from the table, adding two braces and a bar (change from 'original' condition to the current configuration) changes the first resonant frequency by about 26% percent. Adding two more braces (from Model O to Model B) results in increase of the first resonant frequency by about 47% percent. Adding more braces to this configuration does affect the frequency. Essentially, from the resonant frequencies point of view, Models B and C are almost identical. Therefore, the comparative time history analysis was limited to Model O, Model A and Model B.

An analysis of the numerical results leads to the following conclusions. The current reinforcement is not as effective as it was intended to be. As presented in left and middle images of Fig. 14, the stress concentration at the bottom of the reinforced model is even greater than that in a model without any reinforcement. The same conclusion can be drawn from the displacements on top of the portal shown in Fig. 15. The current reinforcement failed to reduce the displacements on top of the portal. Moreover, the peak displacement of Model A is greater than that of Model O. Adding two more braces to Model A results in Model B that has much better performance as presented in the right image of Fig. 14. These braces also helped to reduce peak displacement on top of the portal, as presented in the right image of Fig. 15.

Table 2 – Models with various reinforcement

Model	Description of reinforcement	Color of braces	Resonant frequencies, Hz 1	2	3	4
Model O (‘original’ condition)	No reinforcement	NA	1.37	1.92	3.01	5.50
Model A (current condition)	Two braces and bar	Purple	1.73	2.01	3.52	5.54
Model B	Four braces and bar	Purple, red	2.02	2.06	4.00	5.66
Model C	Eight braces and bar	Purple, red, and cyan	2.04	2.09	4.13	5.67

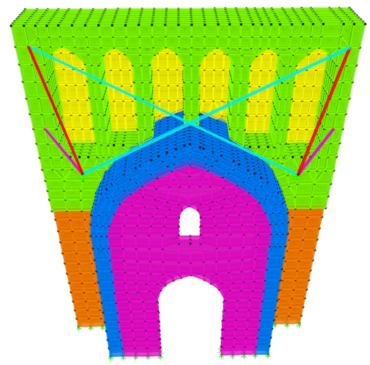

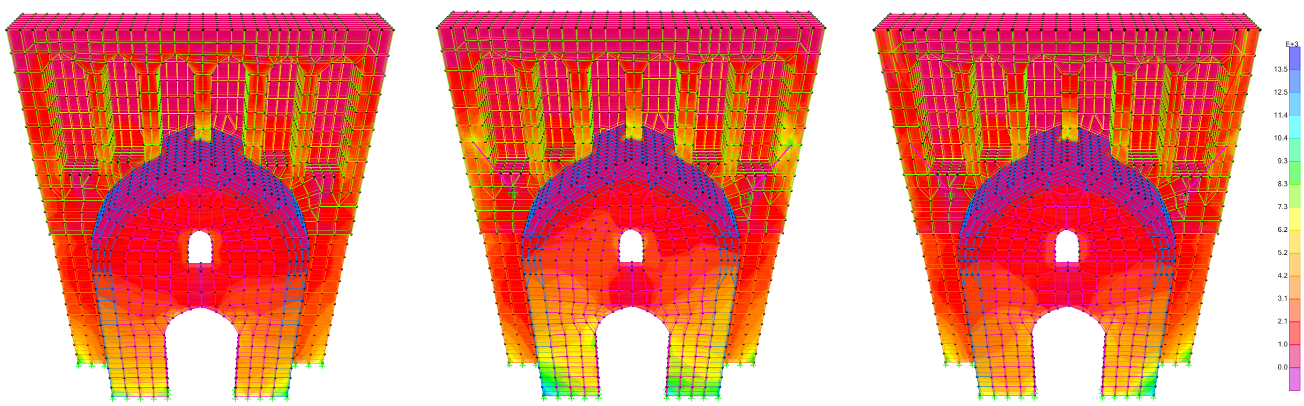

Model O Model A Model B

Fig. 14 – Envelope of tension stresses (S33) for time history runs

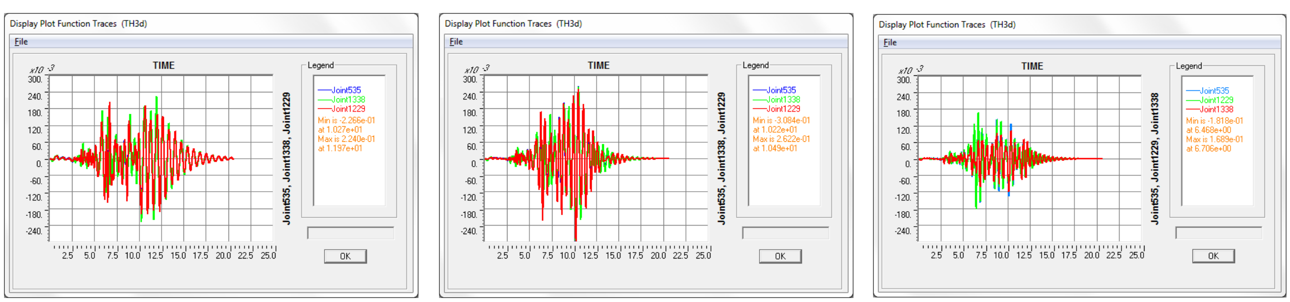

Model O Model A Model B

Fig. 15 – Displacements on top of portal (blue line – mid-span; green and red lines – outer sides)

7. Conclusions

The study (results of which are presented herein) show the advantage of using laser scanning for accurate documentation of the geometry of a historic monument. Structural anomalies of the monument’s current condition were analyzed and will be utilized in follow-up monitoring expeditions.

It was shown that the portal has a significant residual drift that needs to be monitored to ensure that it is not progressing. It was also advised to proceed with the installation of laser targets to increase the accuracy of monitoring. The inclination of the portal increases from south to north with the maximum differential displacement of 0.6 m at the top north corner. A large crack documented by the scanner most likely completely separates the portal from the main structure.

From the analysis of the point cloud it was concluded that the pre-tensioned rods did not reveal any sagging. This serves as evidence that a tension force is still present in the rods. One of the pretension rods applied force in a weak direction of the reinforcement member that resulted in local failure of the member, and as such it cannot serve its function.

The inner globe has some imperfections with the north half at a higher elevation than that on the south side. The latter can be a result of soil settlement on the south side of the building. Periodic monitoring by laser scanning is planned for future investigations.

From a comparative analysis of several numerical models the following was concluded. The current reinforcement is not as effective as it was intended to be. The stress concentration at the bottom of the reinforced model is even greater than that in a model without reinforcement. The same conclusion can be drawn from the displacements on top of the portal. The current reinforcement failed to reduce the displacements on top of the portal. Moreover, the peak displacement of Model A is greater than that of Model O. Adding two more braces to Model A results in Model B that has a better seismic performance.

More analysis aiming at better reinforcement strategies are planned for future studies. These studies will include tests of the masonry wall, ambient vibration studies to estimate resonant frequencies at low excitations, and more detailed numerical models analyzed in a nonlinear time history simulation. The old reinforcement and any new reinforcement attracts the forces and creates stress concentration points. Therefore, these forces need to be properly distributed at the point where they come into contact with the masonry.

8. Acknowledgements

Special thanks are due to BNZ and Smart Scanning Solutions (SSS) (both from Uzbekistan) for providing a laser scanner and financial support of this pilot program. Support from staff of Ministry of Culture and Physical Education in providing access to the historic monuments is greatly appreciated. This project could not be successfully completed without the hard work and technical support of BNZ's and SSS's staff.

9. Copyrights

10. References

[1] Shakhzod Takhirov, Khalid M. Mosalam, Mohamed A. Moustafa, Liliya Myagkova, and Brian Quigley (2015). LASER SCANNING, MODELING, AND ANALYSIS FOR DAMAGE ASSESSMENT AND RESTORATION OF HISTORICAL STRUCTURES. COMPDYN 2015. 5th ECCOMAS Thematic Conference on Computational Methods in Structural Dynamics and Earthquake Engineering. M. Papadrakakis, V. Papadopoulos, V. Plevris (eds.). Crete Island, Greece, 25–27 May 2015.

[2] Leica Geosystems, AG. (2015): Cyclone Version 9.1.

[3] Computers and Structures, Inc. (CSI), 2014. SAP2000 Ultimate Version 16.1.1. Structural Analysis Program.

[4] Pande, G. N., Liang, J. X., and Middleton, J. (1989). "Equivalent elastic moduli for brick masonry." Comput. Geotech., 8(3), 243–265.

[5] Anthoine, A. (1995). "Derivation of the in-plane elastic characteristics of masonry through homogenization theory." Int. J. Solids Struct., 32(2), 137–163.

[6] Wang, G., Li, S., Nguyen, H., and Sitar, N. (2007). "Effective elastic stiffness for periodic masonry structures via eigenstrain homogenization." J. Mater. Civ. Eng., 10.1061/(ASCE)0899-1561(2007)19:3(269), 269–277.

[7] BRITISH STANDARDS INSTITUTION. BS EN 1996–1–1: Eurocode 6 – Design of masonry structures. General rules for reinforced and unreinforced masonry structures. BSI, 2005. Including NA to BS EN 1996-1-1:2005+A1:2012.

[8] Peralta, N., Mosalam, K., and Li, S. (2016). "Multiscale Homogenization Analysis of the Effective Elastic Properties of Masonry Structures." J. Mater. Civ. Eng. , 10.1061/(ASCE)MT.1943-5533.0001561 , 04016056.

[9] http://ngawest2.berkeley.edu/site

[10] Seismic code of Uzbekistan, KMK 2.01.03-96 "Norms and Regulations for Construction in Seismic Zones", Tashkent, Uzbekistan,1996, 125 pages (in Uzbek and Russian).